PROCEEDINGS OF SCIENCE

Search for a new scalar or pseudoscalar heavy Higgs Boson using production of four top quarks at the Large Hadron Collider

Chainika Chauhan[a,*] **on behalf of the ATLAS Collaboration**

[a] *Faculty of Mathematics and Physics, Charles University, V Holešovičkách 2, Prague, Czech Republic*

E-mail: chainika.chauhan@cern.ch

The Standard Model (SM) of particle physics has been remarkably successful in explaining a wide range of experimental observations. However, there are several fundamental questions which remain unanswered, such as the incorporation of gravity into the SM, radiative corrections to mass of Higgs boson, the matter-antimatter asymmetry, and the existence of viable dark matter candidates. One potential solution to these challenges is extending the SM by introducing an additional Higgs doublet. This analysis investigates the presence of a neutral scalar (H) or pseudoscalar (A) heavy Higgs boson, as predicted by the Two-Higgs-Doublet Model (2HDM), produced in association with a pair of top quarks and subsequently decaying into a top-quark pair. The analysis is based on proton-proton (pp) collisions at a center-of-mass energy of 13 TeV, using data collected by the ATLAS detector at the Large Hadron Collider (LHC). Events with exactly one or two oppositely charged leptons (electrons or muons) in the final state are considered. To enhance the modeling of the dominant background from top-antitop production with additional jets, data-driven corrections are applied. A powerful Graph Neural Network classifier is employed to improve signal-background discrimination. This search is further combined with a previous ATLAS analysis in the multilepton channel to set upper limits on the production cross section of H/A bosons with masses ranging from 400 GeV to 1000 GeV in the alignment limit. Additionally, constraints are applied on a model predicting the existence of a color-octet scalar, known as a sgluon, which decays into a pair of top quarks.

Proceedings of the Corfu Summer Institute 2024 "School and Workshops on Elementary Particle Physics and Gravity" (CORFU2024)
25 August - 27 September, 2024
Corfu, Greece

*Speaker

ISSN 1824-8039. Published by SISSA Medialab.

ATL-PHYS-PROC-2025-025
31 March 2025

PoS(CORFU2024)082

1. Introduction

The Standard Model (SM) of Particle Physics became complete in its set of elementary particles following the discovery of the Higgs boson by the ATLAS [1] and CMS [2] experiments at CERN [3, 4]. However, despite this completeness, the SM still faces significant challenges due to the Higgs boson, including the hierarchy problem, baryogenesis, and various experimental anomalies. Notably, the loop quantum corrections in the mass of the Higgs boson lead to the quadratic divergences [5]. This indicates that the SM is fundamentally incomplete in addressing such phenomena and suggests the presence of new physics. One possible approach to address these challenges is to extend the Higgs sector such as in Two-Higgs-Doublet Model (2HDM) [6], hMSSM [7–9] and and those incorporating Higgs triplets [10–15]. In these proceedings, a minimal extension of the Higgs sector is considered by introducing an additional Higgs doublet, following the framework of the Type II 2HDM. In this model, there are two complex doublets of Higgs which give rise to a total of eight degrees of freedom in the scalar sector. But after spontaneous symmetry breaking (SSB), three degrees of freedom are absorbed by the $W^{\pm}$ and Z bosons, providing their longitudinal polarization components and leaving only five physical Higgs bosons. This model predicts the existence of two charged Higgs bosons ($H^{\pm}$), a neutral CP-odd Higgs boson (A), and two neutral CP-even Higgs bosons (H, h), where h is the lighter one and identified as the 125 GeV Higgs boson in the SM. The heavy Higgs bosons, both the neutral scalar (H) and pseudoscalar (A), can introduce new sources of CP violation, which are essential for successful baryogenesis. Additionally, they can contribute to canceling the divergences that emerge in radiative corrections to the mass of the SM Higgs boson. There are five parameters including the mixing angle of the two CP-even Higgs bosons as α, the ratio of the vacuum expectation values of the two Higgs doublets as $\tan\beta$, and the three masses of the Higgs bosons ($m_{H^{\pm}}$, $m_{H/A}$, m_h). Similar direct and indirect searches for these heavy-scalar/pseudoscalar Higgs bosons have been performed by the ATLAS and CMS experiments in the past [16–21].

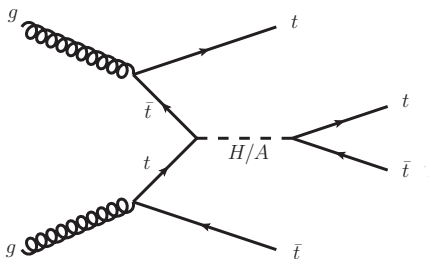

Figure 1: Feynman diagram showing the production of a scalar/pseudoscalar Higgs boson in four-top-quark final state ($t\bar{t}H/A \to t\bar{t}t\bar{t}$) [22].

In these proceedings, a search for the scalar (H) or pseudoscalar (A) heavy Higgs boson (decaying to a pair of top quarks, $t\bar{t}$) produced in association with a pair of top quarks ($t\bar{t}H/A \to t\bar{t}t\bar{t}$) is presented in the alignment limit (where lighter CP-even Higgs boson h couplings are same as SM Higgs boson) [22], as illustrated in Figure 1. The mass of the hypothetical heavy Higgs boson ($m_{H/A}$) is considered to be in the range of 400 to 1000 GeV with a step of 100 GeV. Events with a single lepton (electron or muon) or a pair of oppositely charged leptons (1L/2LOS) are selected as final-state particles. The analysis employs the Run-2 dataset recorded with the ATLAS detector at LHC, corresponding to an integrated luminosity of 139 fb^{-1} [23] at a center-of-mass energy of $\sqrt{s}$ = 13 TeV in proton-proton (pp) collisions. The interference effects of SM $t\bar{t}t\bar{t}$ are not taken into account. The Monte Carlo (MC) samples are generated for all background and signal processes. Separate samples are not generated for $t\bar{t}A \to t\bar{t}t\bar{t}$ as the kinematic differences

between $t\bar{t}H \to t\bar{t}t\bar{t}$ and $t\bar{t}A \to t\bar{t}t\bar{t}$ are found to be less than 1%. No mixing between scalar and pseudoscalar Higgs boson is considered. It is observed from few studies that the event kinematics of interest is independent of the value of β at leading order calculation. The same analytical approach is employed to establish constraints on the sgluon model, which predicts the production of a pair of color-octet scalars, referred to as scalar gluons, decaying into top-antitop quark pairs [24].

2. Object selection and Event categorisation

Events are classified on the basis of leptons, jets, and b-tagged jet multiplicity as shown in Figure 2. The events are preselected if they contain exactly one or two opposite-charge leptons (only electrons or muons) collected using single-lepton triggers with a transverse momentum (p_{T}) threshold of 28 GeV after applying data quality requirements [25]. The jets are constructed using the anti-k_t algorithm [26, 27] with a radius parameter of 0.4, referred to as small-R jets. The jet-vertex tagger [28] is used to mitigate the effect of pileup. The b-jets are identified using the DL1r algorithm [29]. A selected event containing exactly one (two opposite-charge) lepton(s) should have jet multiplicity between seven (7j) to at least ten ($\geq$ 10j) for the single-lepton (1L) channel and five (5j) to at least eight ($\geq$ 8j) for the dilepton opposite sign (2LOS) channel, with at least two of them as b-tagged jets passing a working point of 70%.

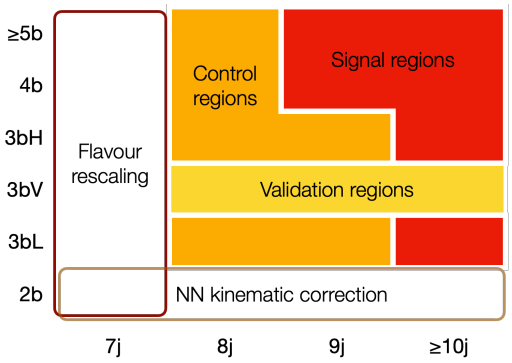

Figure 2: Illustration of events categorised into signal (SR), control (CR), and validation (VR) regions for the 1L channel, based on jet multiplicities (x-axis) and b-tagging criteria (y-axis). Highlighted rectangles represent analysis regions used for deriving flavour rescaling and Neural Network (NN) kinematic corrections [22].

3. Estimation of Background

The primary background influencing the signal process $t\bar{t}H/A \to t\bar{t}t\bar{t}$ originates from $t\bar{t}$+jets. The production of $t\bar{t}$ along with the additional jets that originate from sources other than the direct decay of the top quark, is referred to as $t\bar{t}$+jets. The remaining background consists of the production of SM four-top quarks ($t\bar{t}t\bar{t}$), $t\bar{t}$ produced in association with a Higgs boson ($t\bar{t}H$) or a weak boson ($t\bar{t}W$, $t\bar{t}Z$), single-top-quark events, diboson production, etc. and represents only 8% of the data in the signal region. The $t\bar{t}$ events that include additional jets that are matched to the b-hadron are classified as $t\bar{t}$+$\geq 1b$. Events that do not fall under $t\bar{t}$+$\geq 1b$ but contain at least one additional particle jet associated with c hadron(s) are classified as $t\bar{t}$+$\geq 1c$ events. The $t\bar{t}$+$\geq 1b$ and $t\bar{t}$+$\geq 1c$ events together are known as $t\bar{t}$+HF events (HF stands for heavy flavour). In addition, events that do not fall under $t\bar{t}$+$\geq 1b$ or $t\bar{t}$+$\geq 1c$, are classified as $t\bar{t}$+light events.

However, some previous searches have observed that the overall normalization of the $t\bar{t}$+HF jets is underestimated [30, 31], and certain kinematic mismodelings occur in the high jets p_{T} regime [32]. To address this issue, data-driven corrections are implemented for $t\bar{t}$+jets in two sequential steps derived from orthogonal regions, as shown in Figure 2. Firstly, the ratio of post-fit

to pre-fit yield is determined using a profile likelihood fit (discussed in Section 6), in which the fitted observable is the sum of the pseudo-continuous b-tagging score of the third and fourth jets, ordered in the descending score. This ratio serves as a normalization factor and is applied to $t\bar{t}$+jets. Then, a feed-forward neural network (NN) [33, 34] is trained to correct the kinematic mismodeling observed in $t\bar{t}$+jets. The NN acts as a binary classifier between the simulated $t\bar{t}$+jets and the data. The simulated non-$t\bar{t}$+jets events are labeled as data with negative weights. The output of the NN $o(\mathbf{x})$ as a function of the input vector $(\mathbf{x})$ can be expressed as the a posteriori Bayesian probability of the data $P_{\text{data}}(\mathbf{x})$ and the simulations $P_{\text{MC}}(\mathbf{x})$:

$$o(\mathbf{x}) = P(\text{data}|\mathbf{x}) = \frac{\alpha_{\text{data}} P_{\text{data}}(\mathbf{x})}{\alpha_{\text{data}} P_{\text{data}}(\mathbf{x}) + \alpha_{\text{MC}} P_{\text{MC}}(\mathbf{x})} \tag{1}$$

where the fractions of data and simulated events used for the training are denoted by α_{data} and α_{MC}, respectively, satisfying the condition $\alpha_{\text{data}} + \alpha_{\text{MC}} = 1$. After minimising the exponential loss function (L),

$$L = P_{\text{data}}(\mathbf{x}) e^{-\frac{o(\mathbf{x})}{2}} + P_{\text{MC}}(\mathbf{x}) e^{\frac{o(\mathbf{x})}{2}} \tag{2}$$

with respect to $o(\mathbf{x})$, NN reweighting factors are derived as,

$$w(\mathbf{x}) = e^{o(\mathbf{x})} \tag{3}$$

and applied to the $t\bar{t}$+jets resulting in a significant enhancement in the agreement between data and the MC prediction.

4. Signal Extraction against Background

Since $t\bar{t}$+jets form an irreducible background for the signal process, distinguishing the signal from the background is essential. Graph Neural Networks (GNNs) [35] built with the library PyTorch [36], utilize graphs to efficiently model the kinematics of an event, where nodes represent reconstructed objects, and edges depict connections or relationships between node pairs. The mass-parameterised [37] GNN acts as a binary classifier between the signal process at all assumed masspoints: $t\bar{t}H/A \to t\bar{t}t\bar{t}$ and the background: $t\bar{t}$+jets. Training is carried out separately for the 1L (2LOS) channel with at least 9(7) jets and at least three b-tagged jets obtained with an average efficiency of 70% inclusively. The performance of the GNN in distinguishing the signal from the background is depicted in Figure 3. It is observed that GNN performs better for large masses of heavy Higgs bosons.

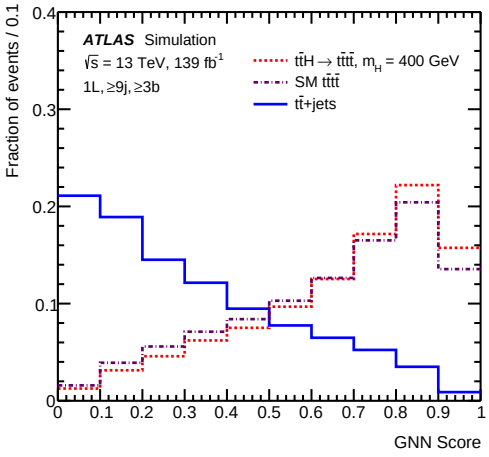

Figure 3: The GNN distribution compared for $t\bar{t}H/A \to t\bar{t}t\bar{t}$, SM $t\bar{t}t\bar{t}$ and $t\bar{t}$+jets at $m_{H/A}$ = 400 GeV in the 1L channel with ≥ 9 jets and ≥ 3 b-tagged jets. [22]

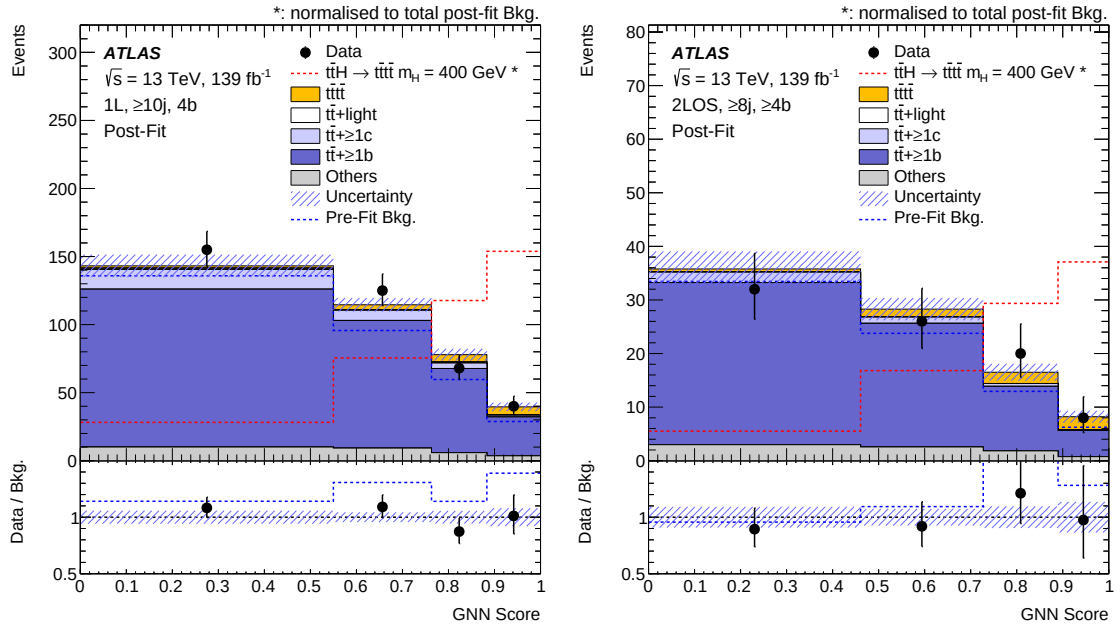

(a) 1L **(b)** 2LOS

Figure 4: Post-fit distributions of the output of GNN evaluated at $m_H = 400$ GeV in the (a) 1L region with ≥ 10 jets and four b-tagged jets and (b) 2LOS region with ≥ 8 jets and ≥ 4 b-tagged jets. The signal is shown with red dashed line normalised to total post-fit background. The fit is performed with the background-only hypothesis [22].

5. Systematic Uncertainties

Systematic uncertainties originate from limitations or biases within the measurement process, the experimental setup, or theoretical model. These encompass experimental uncertainties related to object reconstruction and calibration, such as jet energy scale, jet energy resolution [38], uncertainty in luminosity measurements, taken as 1.7% [23] and b-tagging calibrations [39–41]. Theoretical modeling uncertainties arising from approximations and assumptions in the modeling of signal [42] and background processes, such as the choice of parton distribution functions, matrix element generator, and higher-order QCD corrections are considered. A normalization uncertainty of 50% is attributed to $t\bar{t}$+≥1b and $t\bar{t}$+≥1c, whereas $t\bar{t}$+light is assigned an uncertainty of 5%. Other minor backgrounds are also assigned normalization uncertainties. In addition, uncertainties arising from data-driven background estimations, finite training datasets, are also taken into account. Among all the uncertainties considered, the $t\bar{t}$ modeling uncertainties are found to have the greatest impact on the results.

6. Statistical Analysis

A binned profile likelihood fit is performed for each hypothesized mass of the heavy Higgs boson, simultaneously incorporating all signal and control regions across both decay channels to detect the potential presence of a signal. The profile likelihood function ($\mathcal{L}$) is formulated as the

overall product of the Poisson ($\mathcal{P}$) and Gaussian probability density ($\mathcal{G}$) terms in all bins in the distributions of CR and SR,

$$\mathcal{L}\left(\vec{n}|\mu,\vec{\theta}\right) = \prod_{r\in\text{region}}\prod_{i\in\text{bin}}\mathcal{P}\left(n_{i,r}|\mu S_{i,r}(\vec{\theta}) + B_{i,r}(\vec{\theta})\right) \times \prod_{j\in\text{NP}}\mathcal{G}\left(\theta_j\right) \tag{4}$$

where $\vec{n}$ represents the data vector, μ represents the signal strength which is a parameter of interest (POI) defined as the ratio of the measured cross section of SM $t\bar{t}t\bar{t}$ to a reference cross section (12 fb^{-1}), $\vec{\theta}$ corresponds to the constrained nuisance parameters associated with systematic uncertainties affecting signal and background yields. The quantities $n_{i,r}$, $S_{i,r}$, and $B_{i,r}$ denote the data, signal, and background yields in bin i of the analysis region r, respectively.

Figure 4 presents the post-fit distribution of the GNN in the fitted region with the highest sensitivity to the signal, demonstrating a satisfactory consistency between the data and the MC prediction. The current search in 1L/2LOS is combined with the previous search conducted in the multi-lepton (2LSS/ML) channel [19]. This allows for more precise results. The two searches are statistically independent because of the distinct lepton selection criteria applied in each case. Their combination is performed using a simultaneous profile likelihood fit, integrating all SRs and CRs from both final states while fully correlating all systematic uncertainties. However, the primary background in 2LSS/ML arises from $t\bar{t}W$. Consequently, the uncertainties associated with $t\bar{t}$+jets and $t\bar{t}W$ are treated as uncorrelated.

7. Results and Conclusion

No significant excess of events from the SM prediction is observed in the case of 2HDM. As a result, the upper limits on the POI are set using the CL$_s$ method [49, 50].

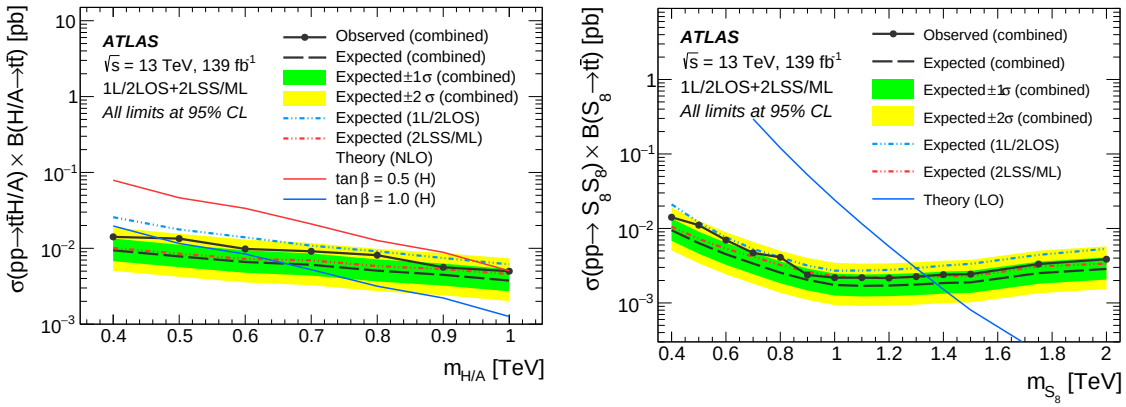

(a) $t\bar{t}H/A \to t\bar{t}t\bar{t}$ **(b)** $S_8S_8 \to t\bar{t}t\bar{t}$

Figure 5: Expected and observed 95% CL upper limits on the cross section times branching fraction (a) $\sigma(pp \to t\bar{t}H/A) \times BR(H/A \to t\bar{t})$ as a function of $m_{H/A}$, (b) $\sigma(pp \to S_8S_8) \times BR(S_8 \to t\bar{t})$ as a function of m_{S_8}, obtained from the combination of the 1L/2LOS and 2LSS/ML final states. The blue and red dashed lines represent expected limits obtained from the individual 1L/2LOS and 2LSS/ML channels, respectively. Theoretical predictions at next-to-leading order in QCD for two values of $\tan\beta$ are shown for H/A boson [43–48] while one is shown for sgluon [22].

The observed and expected upper limits at 95% CL_s are excluded for the $t\bar{t}H/A \to t\bar{t}t\bar{t}$ production cross section for the combined channel (1L/2LOS +2LSS/ML) as shown in Figure 5 (a). The combined expected limits are consistently lower than those obtained from the individual channels, resulting in a 19% improvement over using only the multi-lepton channels, as more signal events contribute to the analysis. Furthermore, 95% CL_s lower limits are excluded for $\tan\beta$ as a function of the mass of the hypothetical Higgs boson. At 0.4(1.0) TeV, $\tan\beta$ values below 1.7(0.7) are excluded when H and A contribute to the final state, below 1.2(0.5) when only H contributes and below 1.5(0.5) when only A contributes.

The analysis approach applied in the search for a 2HDM signal is also utilized to place constraints on the s-gluon model, which predicts the production of a pair of scalar states, S_8 (color-octet with respect to $SU(3)_c$), subsequently decaying into a pair of top quarks. The targeted signal process is $S_8S_8 \to t\bar{t}t\bar{t}$. The hypothesized mass of the s-gluon spans from 0.4 to 1.5 TeV with an increment of 0.1 TeV along with additional values at 1.75 and 2.0 TeV. The observed and expected upper bounds at 95% CL_s are excluded for the production of the $S_8S_8 \to t\bar{t}t\bar{t}$ process in the combined channel as shown in Figure 5 (b). The observed limits are slightly weak for $m_{S_8} \geq 1.0$ TeV. This is because for masses greater than 1.0 TeV, the binary classifiers are optimized for a mass of 1.0 TeV. The combined expected limits show an improvement of 26% as compared to when using only the multi-lepton channels. The sgluon masses $m_{S_8} \leq 1.3$ TeV are excluded.

Acknowledgements

This project has received funding from the Charles University Primus Research Program (Project No 21/SCI/017).

References

[1] ATLAS Collaboration, *The ATLAS Experiment at the CERN Large Hadron Collider*, JINST 3 (2008), S08003.

[2] CMS Collaboration, *The CMS experiment at the CERN LHC*, JINST 3 (2008), S08004.

[3] ATLAS Collaboration, *Observation of a new particle in the search for the Standard Model Higgs boson with the ATLAS detector at the LHC*, Phys. Lett. B 716 (2012) 1-29, arXiv:1207.7214 [hep-ex].

[4] CMS Collaboration, *Observation of a new boson at a Mass of 125* GeV *with the CMS Experiment at the LHC*, Phys. Lett. B 716 (2012) 30, arXiv:1207.7235 [hep-ex].

[5] L. Susskind, *Dynamics of Spontaneous Symmetry Breaking in the Weinberg-Salam Theory* Phys. Rev. D 20 (1979) 2619.

[6] G. C. Branco et al., *Theory and phenomenology of two-Higgs-doublet models*, Phys. Rept. 516 (2012) 1, arXiv:1106.0034 [hep-ph].

PoS(CORFU2024)082

[7] L. Maiani, A. D. Polosa and V. Riquer, *Bounds to the Higgs Sector Masses in Minimal Supersymmetry from LHC Data*, Phys. Lett. B 724 (2013) 274, arXiv:1305.2172 [hep-ph].

[8] A. Djouadi et al., *The post-Higgs MSSM scenario: Habemus MSSM?*, Eur. Phys. J. C 73 (2013) 2650, arXiv:1307.5205 [hep-ph].

[9] A. Djouadi, L. Maiani, A. Polosa, J. Quevillon and V. Riquer, *Fully covering the MSSM Higgs sector at the LHC*, JHEP 06 (2015) 168, arXiv:1502.05653 [hep-ph].

[10] T. D. Lee, *A Theory of Spontaneous T Violation*, Phys. Rev. D 8 (1973) 1226 ed. by G.Feinberg.

[11] T. P. Cheng and L.-F. Li, *Neutrino Masses, Mixings and Oscillations in $SU(2) \times U(1)$ Models of Electroweak Interactions*, Phys. Rev. D 22 (1980) 2860.

[12] J. Schechter and J. W. F. Valle, *Neutrino Masses in $SU(2) \times U(1)$ Theories*, Phys. Rev. D 22 (1980) 2227.

[13] M. Magg and C. Wetterich, *Neutrino Mass Problem and Gauge Hierarchy*, Phys. Lett. B 94 (1980) 61.

[14] G. Lazarides, Q. Shafi and C. Wetterich, *Proton Lifetime and Fermion Masses in an $SO(10)$ Model*, Nucl. Phys. B 181 (1981) 287.

[15] R. N. Mohapatra and G. Senjanović, *Neutrino Masses and Mixings in Gauge Models with Spontaneous Parity Violation*, Phys. Rev. D 23 (1981) 165.

[16] ATLAS Collaboration, *Search for heavy Higgs bosons decaying into two tau leptons with the ATLAS detector using pp collisions at $\sqrt{s}$ = 13 TeV*, Phys. Rev. Lett. 125 (2020) 051801, arXiv:2002.12223 [hep-ex].

[17] CMS Collaboration, *Search for additional neutral MSSM Higgs bosons in the $\tau\tau$ final state in proton-proton collisions at $\sqrt{s}$ = 13 TeV*, JHEP 09 (2018) 007, arXiv:1803.06553 [hep-ex].

[18] ATLAS Collaboration, *Constraints on new phenomena via Higgs boson couplings and invisible decays with the ATLAS detector*, JHEP 11 (2015) 206, arXiv:1509.00672 [hep-ex].

[19] ATLAS Collaboration, *Search for $t\bar{t}H/A \to t\bar{t}t\bar{t}$ production in the multilepton final state in proton-proton collisions at $\sqrt{s}$ = 13 TeV with the ATLAS detector*, JHEP 07 (2023) 203, arXiv:2211.01136 [hep-ex].

[20] ATLAS Collaboration, *Search for heavy neutral Higgs bosons decaying into a top quark pair in 140 fb^{-1} of proton-proton collision data at $\sqrt{s}$ = 13 TeV*, JHEP 08 (2024) 013, arXiv:2404.18986 [hep-ex].

[21] CMS Collaboration, *Search for heavy Higgs bosons decaying to a top quark pair in proton-proton collisions at $\sqrt{s}$ = 13 TeV with the ATLAS detector*, JHEP 04 (2020) 171, arXiv:1908.01115 [hep-ex].

[22] ATLAS Collaboration, *Search for $t\bar{t}H/A \to t\bar{t}t\bar{t}$ production in proton-proton collisions at $\sqrt{s}$ = 13 TeV with the ATLAS detector*, arXiv:2408.17164 [hep-ex].

[23] ATLAS Collaboration, *Luminosity determination in pp collisions at $\sqrt{s}$ = 13 TeV using the ATLAS detector at the LHC*, ATLAS-CONF-2019-021.

[24] L. Darmé, B. Fuks and F. Maltoni, *Top-philic heavy resonances in four-top final states and their EFT interpretation*, JHEP 09 (2021) 143, arXiv:2104.09512 [hep-ex].

[25] ATLAS Collaboration, *ATLAS data quality operations and performance for 2015–2018 data-taking*, JINST 15 (2020) P04003, arXiv:1911.04632 [physics.ins-det].

[26] M. Cacciari, G. P. Salam and G. Soyez, *The anti-k_t jet clustering algorithm*, JHEP 04 (2008) 063, arXiv:0802.1189 [hep-ph].

[27] M. Cacciari, G. P. Salam and G. Soyez, *FastJet User Manual*, Eur. Phys. J. C 72 (2012) 1896, arXiv:1111.6097 [hep-ph].

[28] ATLAS Collaboration, *Performance of pile-up mitigation techniques for jets in pp collisions at $\sqrt{s}$ = 8 TeV using the ATLAS detector*, Eur. Phys. J. C 76 (2016) 58, arXiv:1510.03823 [hep-ex].

[29] ATLAS Collaboration, *ATLAS flavour-tagging algorithms for the LHC Run 2 pp collision dataset*, Eur. Phys. J. C 83 (2023) 681, arXiv:2211.16345 [physics.data-an].

[30] ATLAS Collaboration, *Measurement of $t\bar{t}$ production in association with additional b-jets in the $e\mu$ final state in proton-proton collisions at $\sqrt{s}$ = 13 TeV with the ATLAS detector*, JHEP 01 (2025) 068, arXiv:2407.13473 [hep-ex].

[31] CMS Collaboration, *Inclusive and differential cross section measurements of $t\bar{t}b\bar{b}$ production in the lepton+jets channel at $\sqrt{s}$ = 13 TeV*, JHEP 05 (2024) 042, arXiv:2309.14442 [hep-ex].

[32] ATLAS Collaboration, *Measurements of top-quark pair differential and double-differential cross-sections in the ℓ+jets channel with pp collisions at $\sqrt{s}$ = 13 TeV using the ATLAS detector*, Eur. Phys. J. C 79 (2019) 1028, arXiv:1908.07305 [hep-ex].

[33] L. Garrido and A. Juste, *On the determination of probability density functions by using Neural Networks*, Comput. Phys. Commun. 115 (1998) 25, arXiv:physics/9807018 [physics.data-an].

[34] G. V. Moustakides and K. Basioti, *Training Neural Networks for Likelihood/Density Ratio Estimation*, arXiv:1911.00405 [eess.SP].

[35] P. W. Battaglia et al., *Relational inductive biases, deep learning, and graph networks*, arXiv:1806.01261 [cs.LG].

[36] A. Paszke et al., *PyTorch: An Imperative Style, High-Performance Deep Learning Library* , arXiv:1912.01703 [cs.LG].

[37] P. Baldi, K. Cranmer, T. Faucett, P. Sadowski and D. Whiteson, *Parameterized neural networks for high-energy physics*, Eur. Phys. J. C 76 (2016), arXiv:1601.07913 [hep-ex].

[38] ATLAS Collaboration, *Jet energy scale and resolution measured in proton-proton collisions at $\sqrt{s}$ = 13 TeV with the ATLAS detector*, Eur. Phys. J. C 81 (2021) 689, arXiv:2007.02645 [hep-ex].

[39] ATLAS Collaboration, *ATLAS b-jet identification performance and efficiency measurement with $t\bar{t}$ events in pp collisions at $\sqrt{s}$ = 13 TeV*, Eur. Phys. J. C 79 (2019) 970, arXiv:1907.05120 [hep-ex].

[40] ATLAS Collaboration, *Measurement of the c-jet mistagging efficiency in $t\bar{t}$ events using pp collision data at $\sqrt{s}$ = 13 TeV collected with the ATLAS detector*, Eur. Phys. J. C 82 (2022) 95, arXiv:2109.10627 [hep-ex].

[41] ATLAS Collaboration, *Calibration of the light-flavour jet mistagging efficiency of the b-tagging algorithms with Z+jets events using 139 fb^{-1} of ATLAS proton-proton collision data at $\sqrt{s}$ = 13 TeV*, Eur. Phys. J. C 83 (2023) 728, arXiv:2301.06319 [hep-ex].

[42] J. Butterworth et al., *PDF4LHC recommendations for LHC Run II*, J. Phys. G 43 (2016) 023001, arXiv:1510.03865 [hep-ph].

[43] R. V. Harlander, S. Liebler and H. Mantler, *SusHi: A program for the calculation of Higgs production in gluon fusion and bottom-quark annihilation in the Standard Model and the MSSM*, Comput. Phys. Commun. 184 (2013) 1605, arXiv:1212.3249 [hep-ph].

[44] R. V. Harlander and W. B. Kilgore, *Next-to-next-to-leading order Higgs production at hadron colliders*, Phys. Rev. Lett. 88 (2002) 201801, arXiv:hep-ph/0201206.

[45] R. V. Harlander and W. B. Kilgore, *Higgs boson production in bottom quark fusion at next-to-next-to-leading order*, Phys. Rev. D 68 (2003) 013001, arXiv:hep-ph/0304035.

[46] U. Aglietti, R. Bonciani, G. Degrassi and A. Vicini, *Two-loop light fermion contribution to Higgs production and decays*, Phys. Lett. B 595 (2004) 432, arXiv:hep-ph/0404071.

[47] R. V. Harlander and P. Kant, *Higgs production and decay: Analytic results at next-to-leading order QCD*, JHEP 12 (2005) 015, arXiv:hep-ph/0509189.

[48] R. Bonciani, G. Degrassi and A. Vicini, *On the Generalized Harmonic Polylogarithms of One Complex Variable*, Comput. Phys. Commun. 182 (2011) 1253, arXiv:1007.1891 [hep-ph].

[49] T. Junk, *Confidence level computation for combining searches with small statistics*, Nucl. Instrum. Meth. A 434 (1999) 435, arXiv:hep-ex/9902006.

[50] A. L. Read, *Presentation of search results: The CL_s technique*, J. Phys. G 28 (2002) 2693.

PoS(CORFU2024)082